Power Electronic Devices and Components 12 (2025) 100108

Contents lists available at ScienceDirect

Power Electronic Devices and Components

journal homepage: www.journals.elsevier.com/power-electronic-devices-and-components

Modelling of SiC and GaN transistors based on pulsed S-parameter measurements

Martin Hergt [a,*], Bernhard Hammer [b], Martin Sack [c], Lukas W. Mayer [d], Sebastian Nielebock [a], Marc Hiller [c]

[a] Siemens AG, Erlangen, Germany
[b] ABB AG, Mannheim, Germany
[c] Karlsruhe Institute of Technology, Karlsruhe, Germany
[d] Siemens Österreich AG, Vienna, Austria

ARTICLE INFO

Keywords:
S-parameters
Parameter identification
Device modelling
GaN HEMT
SiC MOSFET

ABSTRACT

For the design of fast-switching inverters a precise model of power semiconductors is required. Based on pulsed S-parameter measurements in the frequency range of 2 MHz to 500 MHz a SiC MOSFET and a GaN HEMT have been characterized. As basis for precise modelling, measurements under varying load conditions have been taken for many operating points covering the pinch-off, ohmic, and active regions. The employed model to describe the transistor uses a circuit comprising 12 circuit elements. Thereby, the elements of the intrinsic transistor vary with the transistor's operating point and parameters describing the influence of the package are considered to be constant. The model parameters have been adjusted iteratively. A comparison of the obtained model with the original S-parameter measurements exhibits an excellent match.

Introduction

Future applications of inverters especially in mobile devices require a design process allowing for a considerable reduction in weight and volume compared to current designs. Such constraints demand for higher switching frequencies of the employed power semiconductors, mostly wide bandgap devices made of silicon carbide (SiC) or gallium nitride (GaN). In the course of the design process, circuit simulations play an important role. Most current device models, however, are sufficiently accurate up to a few MHz only (Endruschat et al., 2018). To derive better models, a setup for characterizing power semiconductors under load conditions in a frequency range between 2 MHz and 500 MHz based on pulsed S-parameter measurements was built and has already been used to characterize a number of devices (Hergt et al., 2019a, 2019b), (Hergt et al., 2024). In Hergt et al. (2024), a silicon transistor for power applications was investigated. It has a comparable structure to conventional RF HEMT, including a package optimized for high switching frequencies with low lead inductance and stray capacitance. Therefore, in the pinch-off and ohmic regions the device can be modelled by means of a simplified equivalent circuit which is well known from modelling of RF transistors (Jarndal, 2006). Ohmic resistors in the intrinsic model are omitted due to its low power losses (Jarndal, 2006). In this work, the RF characteristics of both a SiC Power MOSFET (type C3M0120090J) (6) and a GaN transistor (type GS66504B) (7) are investigated.

A common method for characterizing power semiconductors is the double pulse test (Heckel, 2018). In the course of such a test, a transistor is operated under hard switching conditions connected to an inductive load with a free-wheeling diode, and the device under test (DUT) is characterized by means of time-domain measurements. Especially when testing transistors under high-current conditions, the switch-off process may need to be slowed down to avoid inductive voltage spikes caused by the stray inductance of the leads to the transistor's package. Consequently, the reduced slope of the signals causes a limitation in bandwidth for the applied testing signals. Therefore, the double pulse measurements are especially suitable for measurements in a frequency range below several hundred kilohertz.

The setup for pulsed S-parameter measurements under load conditions enables investigations of the DUT in steady-state using measurements in a frequency range above 2 MHz and, hence, complements other characterization methods.

As the goal of this work is to set up an equivalent circuit allowing for

* Corresponding author.
E-mail address: martin.hergt@siemens.com (M. Hergt).

https://doi.org/10.1016/j.pedc.2025.100108
Received 28 June 2025; Accepted 25 July 2025
Available online 5 August 2025

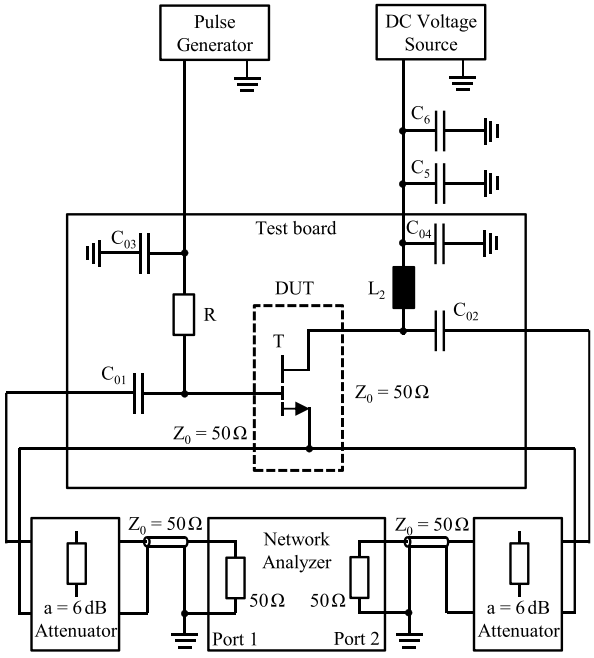

Fig. 1. Schematic of test setup for transistor characterization (DUT).

an accurate RF description of the DUT (Kompa, 1995), dynamic effects like trapping and buffer effects are neglected, as these are relevant in a frequency range well below 2 MHz only.

Experimental setup

The pulsed S-parameter measurements are performed in a test setup allowing for an operation under load conditions (Heckel, 2018). Fig. 1 shows a simplified schematic of the test setup. To test the transistor with a pulsed drain current of up to 300 A, an appropriate coil (L_2) was selected as load. A capacitor bank (C_{04}, C_5, C_6) backed by a DC source serves as voltage source with low inner impedance. A vector network analyzer (VNA), which performs the S-parameter measurements, is decoupled from the test setup by means of the two capacitors C_{01} and C_{02} to protect it against the operating voltage applied to the transistor. The gate signal to control the DUT is generated by a commercial pulse generator. Thereby, the resistor R decouples the RF signal delivered by the network analyzer from the pulse generator output considered as DC source during S-parameter measurements. We selected R = 500 Ω, resulting in a rise time of the gate signal of 30 µs and a fall time of 50 µs, approximately. Due to a short turn-on time and sufficient time between two consecutive measurements, the slightly increased switching losses have only a small impact on the measurements. The input and output connections of the transistor have been matched to 50 Ω.

Notation

Even though we use a very similar notation as in our previous work (Hergt et al., 2024), we repeat the definitions to make the paper more self-contained. We denote matrices by bold uppercase letters and vectors by bold lowercase letters. To refer to the S-parameters measured in the i-th operating point, we write

$$\mathbf{S}^i(\omega) = \begin{bmatrix} S^i_{11}(\omega) & S^i_{12}(\omega) \\ S^i_{21}(\omega) & S^i_{22}(\omega) \end{bmatrix}. \tag{1}$$

Admittance and impedance parameters directly computed from the measurements are denoted in the same way as the S-parameters, using **Y** and **Z**, respectively. We may indicate, whether the operating point i is in the passive region $i \in \mathscr{P}$, the ohmic region $i \in \mathscr{O}$, or in the active region $i \in \mathscr{A}$. The modeled parameters are further marked by a tilde, i.e. $\tilde{\mathbf{S}}^i(\omega)$ signifies the modeled, frequency-dependent S-parameters in the i-th operating point. A subindex i may indicate that the measured or modeled S-, Y- or Z-parameters are pertaining to the intrinsic model of the transistor only, i.e. after de-embedding of the extrinsic parameters.

The parameters of the models are summarized in the vector **p**. To refer to the parameters of the intrinsic model, we may write $\mathbf{p}_\mathrm{i}$, while $\mathbf{p}_\mathrm{e}$ is used to refer to the parameters of the extrinsic model. The parameters are often dependent on the operating point. Then, for the parameters of the i-th operating point, we write $\mathbf{p}^i$.

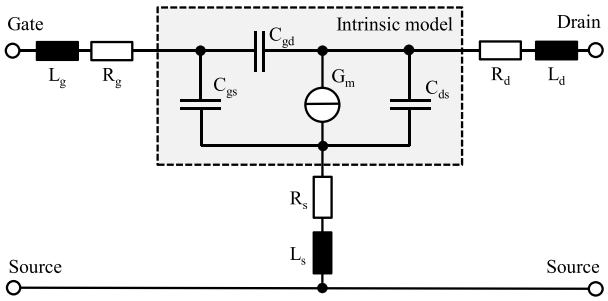

Fig. 2. 10-element model of the small signal behavior of a transistor.

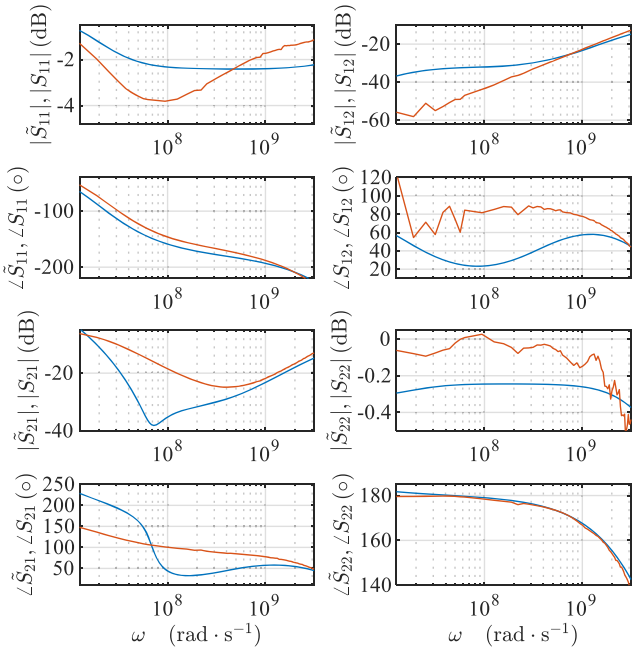

Fig. 3. SiC transistor S-parameters V_{gs} = 11 V, V_{ds} = 3 V. Measurements red, model in blue. 10 Parameter model.

Equivalent circuits of the transistors

10-element model

In the literature, equivalent circuits of different complexity are used to describe transistors. For modelling RF MOSFETs in the pinch-off- and ohmic regions, the 10-element model shown in Fig. 2 is commonly used (Jarndal, 2006). The intrinsic transistor is described by means of its current source G_m and the capacitances C_{gs}, C_{gd}, and C_{ds} between gate, drain, and source, respectively. The extrinsic elements R_g, L_g, R_s, L_s and

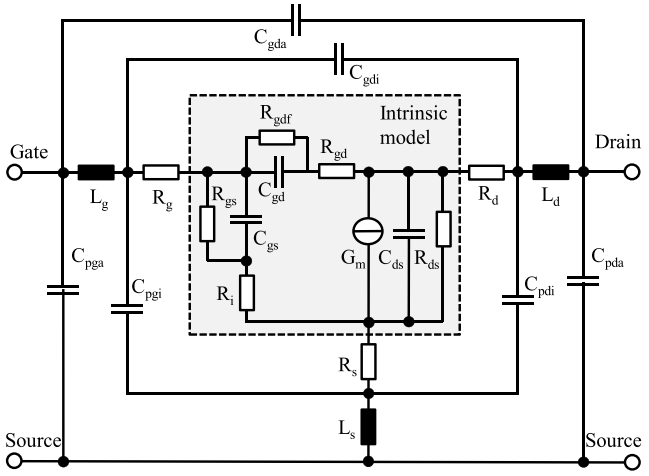

Fig. 4. 21-element model of the small signal behavior of a transistor.

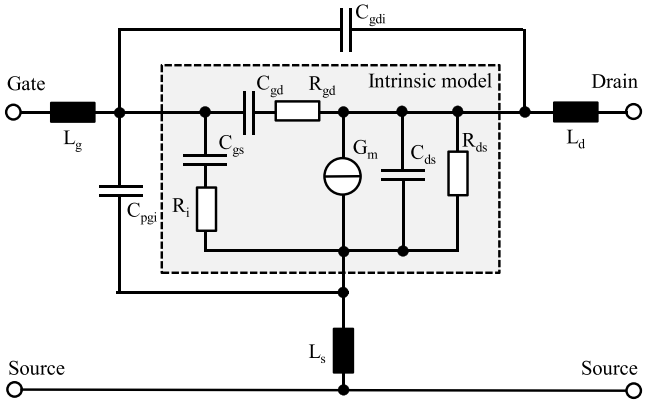

Fig. 5. 12-element model of the small signal behavior of a transistor.

R_d, L_d describe the influence of the package on the signal paths to gate, source, and drain. In our previous work, we successfully applied the 10-element model to describe a silicon transistor (Hergt et al., 2024). In a first attempt to identify a suitable model for the SiC and GaN transistors, the same procedure was applied as in Hergt et al. (2024). However, while the passive region was successfully modeled, the measurements taken in the ohmic and active regions could not be satisfactorily described. Fig. 3 shows the results for an exemplary operating point of the ohmic region. The model obviously exhibits large deviations from the measurements.

12-Element model used for identification

While the 10-element model is very commonly used, a more sophisticated equivalent circuit with 21 elements shown in Fig. 4 is sometimes also applied to describe RF transistors. Compared to the 10-element model, this circuit contains five additional resistors R_i, R_{ds}, R_{gs}, R_{gd}, R_{gdf} in the intrinsic model and six additional capacitances C_{pgi}, C_{pdi}, C_{gdi}, C_{pga}, C_{pda}, C_{gda} in the extrinsic model. As the identification procedure includes non-convex optimization, allowing for additional optimization variables not necessarily yields better results, as the probability of running into local minima increases. Instead, it is better to use an equivalent circuit that has as few parameters as possible, but still can describe all relevant effects.

From the physics of the transistors, we know that the capacitances C_{pga}, C_{pda}, C_{gda} and the resistors R_{gs}, R_{gd}, R_{gdf} have only small influence on the system dynamics. Thus, we neglect these elements. As we now

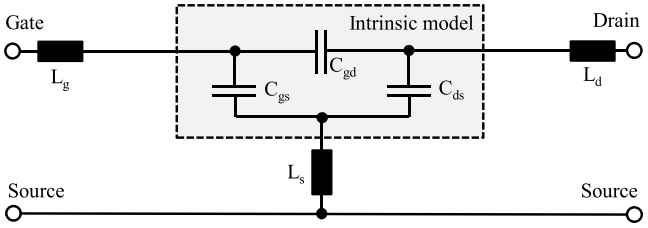

Fig. 6. 6-element model of the small signal behavior of a transistor.

have resistors in the intrinsic model that can represent the losses of the transistor and are allowed to vary in dependence of the operating point, we also neglect the resistors R_g, R_d, R_s in the extrinsic model. Otherwise, if we computed the resistors R_g, R_d, R_s based on the measurements in the pinch-off region as in Hergt et al. (2024), the values for the extrinsic resistors might be overestimated, as they might be used to also represent the losses in the intrinsic model. This might then yield negative resistors in the intrinsic model, when the ohmic and active regions are analyzed. This problem is avoided by neglecting the extrinsic resistors.

Having neglected the extrinsic resistors, the capacitors C_{ds} and C_{pdi} are parallel. Thus, from a mathematical point of view, C_{pdi} gives no additional degrees of freedom and can also be neglected. Later, for the physical interpretation, the minimum value of all C_{ds} can be interpreted to be the capacitance that belongs to the package, i.e. the extrinsic model. Neglecting all these elements from the large 22-element model yields the model with 12 elements shown in Fig. 5.

Parameter identification

Parameter identification in the pinch-off region

To identify the parameters of the equivalent circuit shown in Fig. 5, we again start with the measurements in the pinch-off region, as the current source G_m can then be neglected. The parameters of the intrinsic model

$$\mathbf{p}_{\mathrm{i}}^{i} = \left[C_{\mathrm{gs}}^{i} \quad C_{\mathrm{gd}}^{i} \quad C_{\mathrm{ds}}^{i} \quad R_{\mathrm{i}}^{i} \quad R_{\mathrm{gd}}^{i} \quad R_{\mathrm{ds}}^{i} \right]^{T} \tag{2}$$

and the parameters of the extrinsic model

$$\mathbf{p}_{\mathrm{e}}^{i} = \left[L_{\mathrm{g}}^{i} \quad L_{\mathrm{d}}^{i} \quad L_{\mathrm{s}}^{i} \quad C_{\mathrm{pgi}}^{i} \quad C_{\mathrm{gdi}}^{i} \right]^{T} \tag{3}$$

are at this point still dependent on the operating point.

Instead of directly using the 12-element model, we first apply the very simplified 6-element model shown in Fig. 6, as this allows us to compute initial values for the extrinsic inductances L_{g}^{i}, L_{d}^{i}, L_{s}^{i} and the intrinsic capacitances C_{gd}^{i}, C_{gd}^{i}, C_{ds}^{i} the same way as in Hergt et al. (2024), (Jarndal, 2006). After having computed these initial values, the parameters are optimized for each point in the pinch-off region $i \in \mathscr{P}$, by minimizing the mean square error (MSE) considering the S-parameters measured at N_f discrete frequencies within the considered frequency range:

$$\mathrm{MSE}\left(\mathbf{p}^{i}\right) = \sum_{j=1}^{2} \sum_{k=1}^{2} \sum_{n=1}^{N_{\mathrm{f}}} \frac{\left| \widetilde{S}_{k,j}^{i}(\omega_n, \mathbf{p}^{i}) - S_{k,j}^{i}(\omega_n) \right|^{2}}{N_{\mathrm{f}}}. \tag{4}$$

Then, the five missing parameters are gradually added to the model $\widetilde{\mathbf{S}}^{i}$ and the minimization of (4) is reconducted each time. First, the three resistors R_i, R_{ds}, R_{gd} are added and the optimization process is repeated. Then, the model is completed by the two capacitors C_{pgi} and C_{gdi} and the parameters are again reoptimized. This procedure was chosen, because it helps in avoiding local minima. As the extrinsic parameters are meant to be constant for all operating points, the final extrinsic parameters

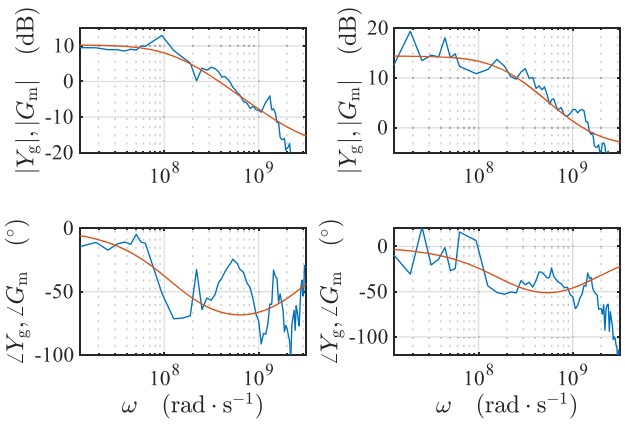

Fig. 7. G_m (red) and Y_g (blue) for the SiC transistor at $V_{gs} = 7$ V, $V_{ds} = 15$ V (left) and at $V_{gs} = 7$ V, $V_{ds} = 4$ V (right).

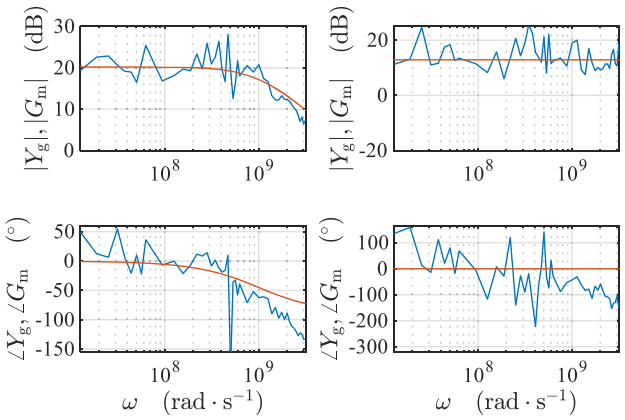

Fig. 8. G_m (red) and Y_g (blue) for the GaN transistor at $V_{gs} = 3$ V, $V_{ds} = 3.5$ V (left) and at $V_{gs} = 3$ V, $V_{ds} = 10$ V (right).

were set by taking the median of the extrinsic parameters that were still dependent on the operating point

$$\mathbf{p}_e = \left[\text{median}\left[L_s^{i\in\mathscr{P}}\right], \ldots, \text{median}\left[C_{gdi}^{i\in\mathscr{P}}\right]\right] = \left[L_g,\ L_d,\ L_s, C_{pgi},\ C_{gdi}\right]. \quad (5)$$

Holding $\mathbf{p}_e$ constant, the optimization procedure was repeated one last time for the pinch-off region, to compute the final intrinsic parameters $\mathbf{p}_i^i$. The results for the pinch-off region were excellent for both the SiC and the GaN transistors.

Parameter identification in the ohmic and active regions

As the extrinsic parameters are meant to be constant for all operating points $\mathbf{p}_e$ and as they were identified using the measurements in the pinch-off region, we can de-embed their effect from the measurements taken in the ohmic and active regions. To do so, we first transform the measured S-parameters to impedance parameters by application of

$$\mathbf{Z}^i = Z_0\left(\mathbf{I} - \mathbf{S}^i\right)^{-1}\left(\mathbf{I} + \mathbf{S}^i\right) \quad (6)$$

with $Z_0 = 50\ \Omega$. Then, we subtract the extrinsic inductors

$$\mathbf{Z}_{i1}^i = \mathbf{Z}^i - s\begin{bmatrix} L_g + L_s & L_s \\ L_s & L_d + L_s \end{bmatrix} \quad (7)$$

and transform the resulting Z-parameters $\mathbf{Z}_{i1}^i$ to admittance parameters $\mathbf{Y}_{i1}^i = \mathbf{Z}_{i1}^{i\,-1}$, from which we de-embed the two extrinsic capacitors

$$\mathbf{Y}_i^i = \mathbf{Y}_{i1}^i - s\begin{bmatrix} C_{pgi} + C_{gdi} & -C_{gdi} \\ -C_{gdi} & C_{gdi} \end{bmatrix} \quad (8)$$

to gain admittance parameters of the intrinsic transistor model $\mathbf{Y}_i^i$. The intrinsic model shown in Fig. 5 can also be represented by following transfer function matrix $\widetilde{\mathbf{Y}}_i^i$ of the intrinsic admittance parameters

$$\widetilde{\mathbf{Y}}_i^i = \begin{bmatrix} \dfrac{sC_{gd}}{sC_{gd}R_{gd}+1} + \dfrac{sC_{gs}}{sC_{gs}R_i+1} & -\dfrac{sC_{gd}}{sC_{gd}R_{gd}+1} \\ G_m^i - \dfrac{sC_{gd}}{sC_{gd}R_{gd}+1} & G_{ds} + sC_{ds} + \dfrac{sC_{gd}}{sC_{gd}R_{gd}+1} \end{bmatrix}. \quad (9)$$

Compared to the intrinsic model in Hergt et al. (2024), (9) is far more complicated. However, the only difference between $\widetilde{Y}_{i,12}^i$ and $\widetilde{Y}_{i,21}^i$ is still the current source G_m^i. Thus, as in Hergt et al. (2024), we compute

$$Y_g^i = Y_{i,21}^i - Y_{i,12}^i \quad (10)$$

and use Y_g^i to identify a model of the current source G_m^i by minimizing

Table 1
Values of the Extrinsic Parameters.

	L_g [nH]	L_d [nH]	L_s [nH]	C_{pgi} [pF]	C_{gdi} [pF]	C_{pdi} [pF]
SiC	6.2479	3.4452	2.4665	0.0319	0	0
GaN	1.4452	1.5076	0.2240	0.0001	0.0001	0

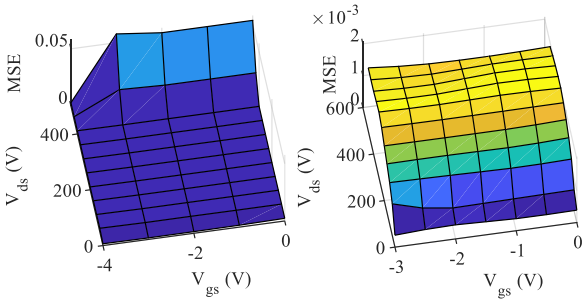

Fig. 9. MSE in pinch-off region for SiC (left) and GaN (right).

$$\sum_{n=1}^{N_f} \frac{\left|G_m^i - Y_g^i(\omega_n)\right|^2}{N_f}. \quad (11)$$

An investigation of Y_g^i thereby motivated us to use following first order transfer function for the current source in the ohmic region, allowing for a frequency-dependent adaptation of G_m^i for each operating point i by an appropriate adjustment of the parameters a and b

$$G_m^i = g_m^i \frac{s + a^i}{s + b^i},\ i \in \mathscr{O}. \quad (12)$$

Figs. 7 and 8 compare resulting models of the current source G_m^i with the respective values Y_g^i in the ohmic and active regions. Fig. 7 shows exemplary results for the SiC transistor and Fig. 8 for the GaN transistor. In the active regions, we applied a simple gain element

$$G_{m,\,GaN}^i = g_m^i,\ i \in \mathscr{A} \quad (13)$$

for the GaN transistor, but stayed with (12) for the SiC transistor. With the current sources identified, we finally compute the intrinsic parameters in each operating point of the ohmic and active regions by minimizing

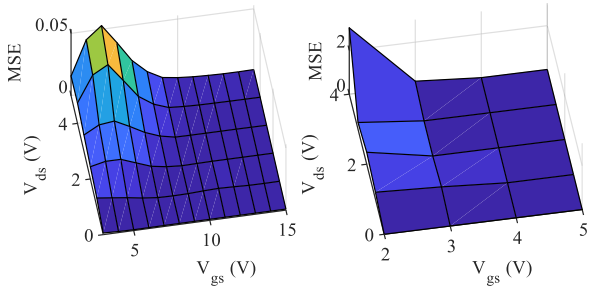

Fig. 10. MSE ohmic region for SiC (left) and GaN (right).

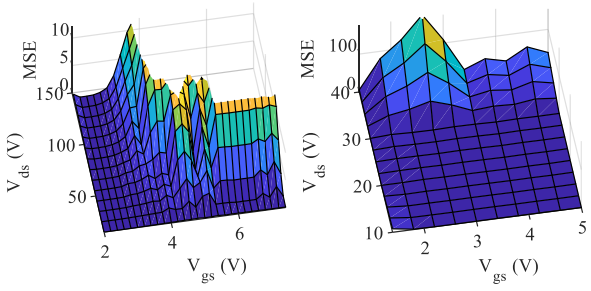

Fig. 11. MSE active region for SiC (left) and GaN (right).

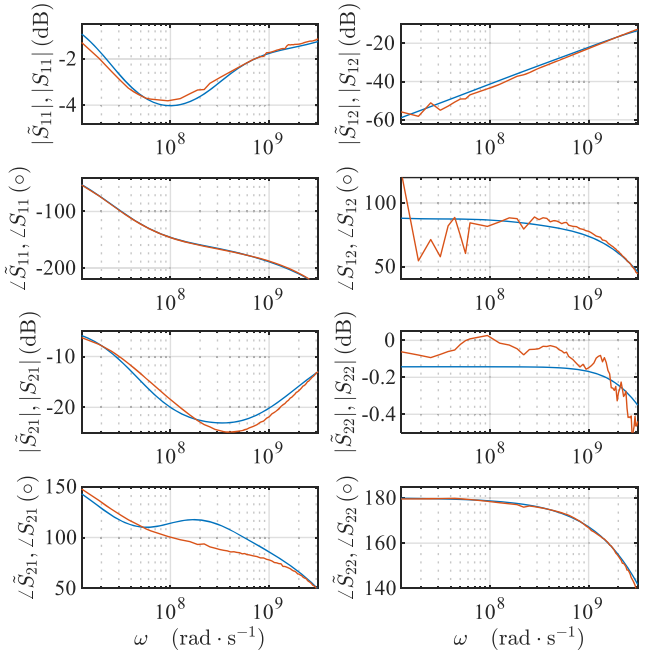

Fig. 12. SiC transistor S-parameters $V_{gs} = 11$ V, $V_{ds} = 3$ V. Measurements red, model in blue.

$$\mathrm{MSE}(\mathbf{p}^i) = \sum_{j=1}^{2}\sum_{k=1}^{2}\sum_{n=1}^{N_f} \frac{\left|\widetilde{S}^i_{i_{k,j}}(\omega_n, \mathbf{p}^i) - S^i_{i_{k,j}}(\omega_n)\right|^2}{N_f}. \tag{14}$$

Results

The resulting extrinsic parameter values of both transistors are given in Table 1 and the MSE of the optimization for both transistors and in all three operating regions are displayed in Figs. 9, 10 and 11. Obviously, the MSE is lowest in the pinch-off region and highest in the active region.

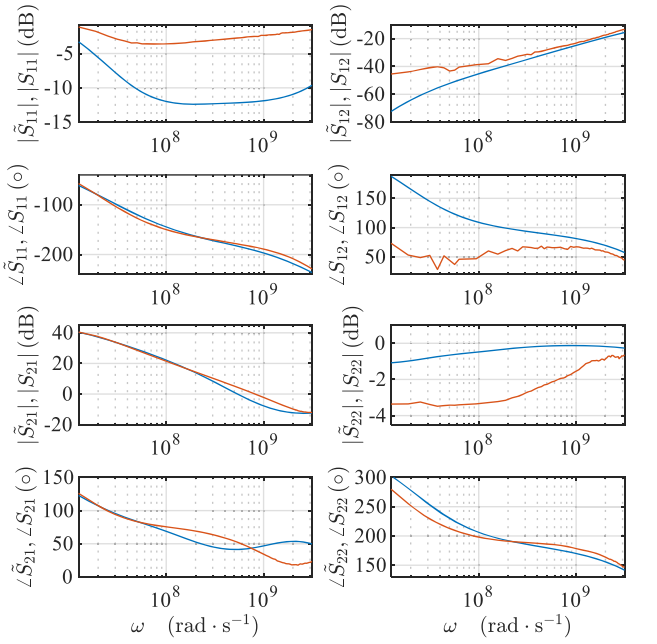

Fig. 13. SiC transistor S-parameters $V_{gs} = 4$ V, $V_{ds} = 60$ V. Measurements red, model in blue.

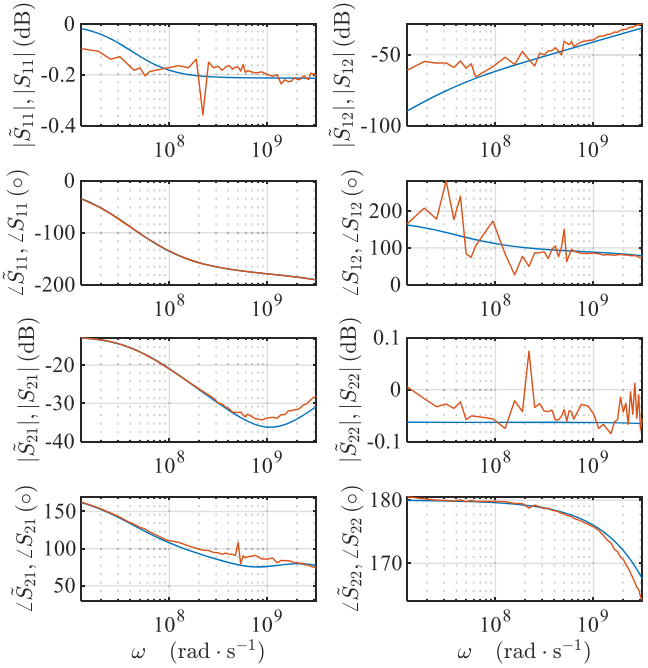

Fig. 14. GaN transistor S-parameters $V_{gs} = 4$ V, $V_{ds} = 3$ V. Measurements red, model in blue.

However, even when the MSE is quite high in the active regions, the fits are actually quite good. The reason for the higher MSE is the generally higher gain in the active region and the accordingly higher noise. Some values are missing in Fig. 11 on the top-right side, because no measurements were taken in this region, as this would damage the transistor.

For the same operating point of the ohmic region shown in Fig. 3, where the 10-parameter model was applied to the SiC transistor, the S-parameters and the corresponding fits are shown in Fig. 12. A comparison of Figs. 3 and 12 clearly shows the improvement that was achieved by application of the 12-element model shown in Fig. 5. For an

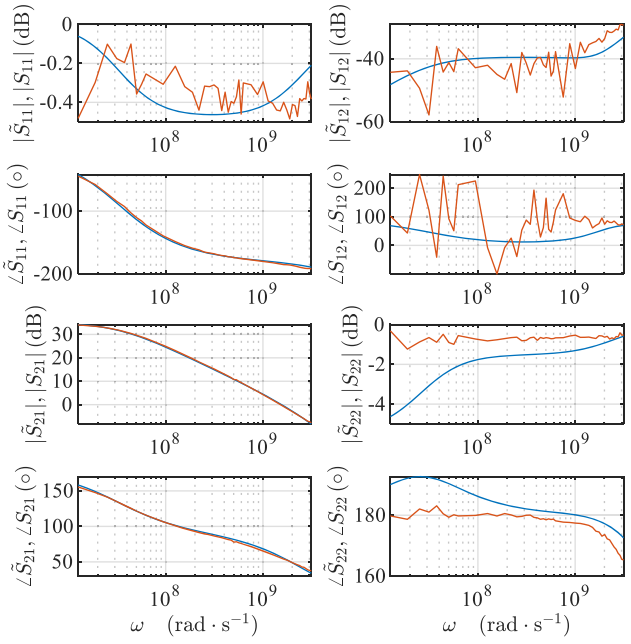

Fig. 15. GaN transistor S-parameters $V_{gs} = 4$ V, $V_{ds} = 20$ V. Measurements red, model in blue.

exemplary operating point in the active region, the measured and modeled S-parameters of the SiC transistor are given in Fig. 13. Corresponding exemplary results for the GaN transistor in the ohmic region are shown in Fig. 14 and for the active region in Fig. 15.

When reading the figures showing the measured and modelled S-parameters, special care needs to be given to the scaling of the axes. Often, were the fit between measurement and model seems poor, this is only an impression given by the axes scaling.

Figs. 16 and 17 show the resulting intrinsic capacitances C_{gs}, C_{ds} and C_{gd} of both transistors in the pinch-off region. The capacitances exhibit the non-linear dependency of the voltages which is well known from the data-sheets. A further validation of the optimization results is given by Figs. 18 and 19, where the capacitances

$$\begin{aligned} C_{iss} &= C_{gd} + C_{gs} \\ C_{oss} &= C_{ds} + C_{gd} \\ C_{rss} &= C_{gd} \end{aligned} \tag{15}$$

are computed from the optimization results with $V_{gs} = 0$ V and compared to the corresponding values given in the data-sheets (6), (7). Obviously, our results are in good accordance with the data-sheets. The deviations in Figs. 18 and 19 can mostly be explained by dispersion effects in the lower frequency range (Jarndal, 2006), in which the data-sheet values were identified. The data sheet values have been identified at a frequency of 1 MHz, while we used the frequency range of 2 MHz to 500 MHz.

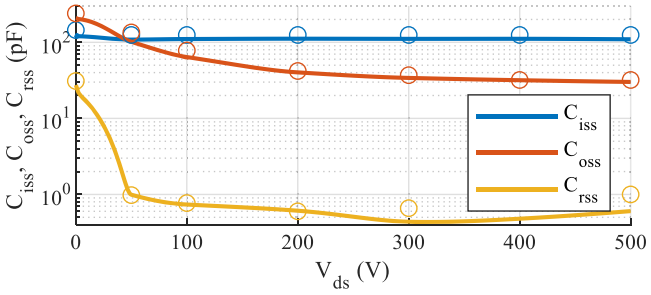

Fig. 18. C_{iss}, C_{oss}, C_{rss} of SiC. Dots from data sheet, lines identified.

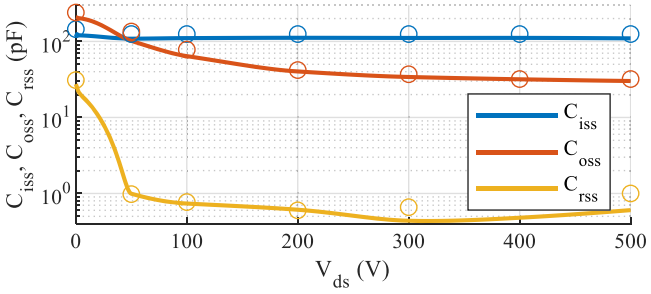

Fig. 19. C_{iss}, C_{oss}, C_{rss} of GaN. Dots from data sheet, lines identified.

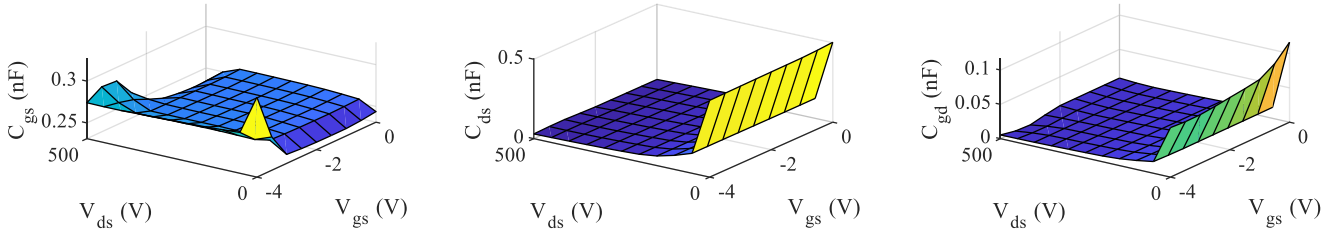

Fig. 16. SiC transistor C_{gs}, C_{ds}, C_{gd} in pinch-off region.

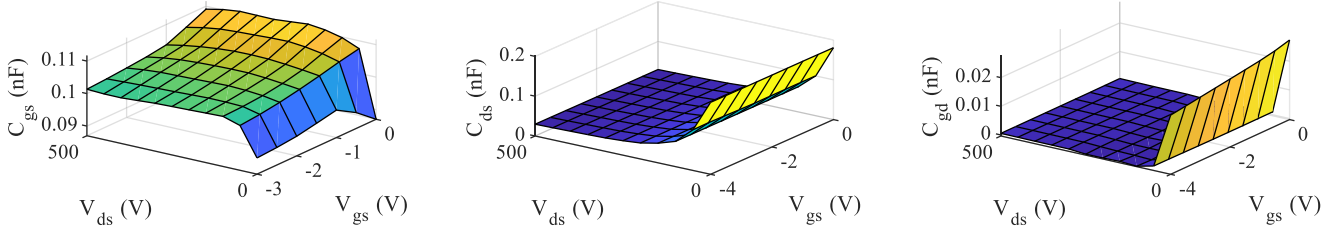

Fig. 17. GaN transistor C_{gs}, C_{ds}, C_{gd} in pinch-off region.

Conclusion

A method for the characterization of a SiC MOSFET and a GaN HEMT based on pulsed S-parameter measurements is presented. Unlike for the Si transistor investigated previously (Hergt et al., 2024), a more detailed model based on 12-elements needs to be applied. Based on the S-parameter measurements the model parameters have been adjusted iteratively.

Crucial for convergence of the iterations are best possible starting values of the parameters. As operating points within the pinch-off region can be described with the model's current source set to zero, starting values are estimated for that operation region first by means of a simplified 6-element equivalent circuit. Then, the optimization is conducted for the pinch-off region using the 12-element model. Thereby, the resulting extrinsic parameters describing the package properties of the transistor are forced to be constant over all operating points. This allows us in a next step to de-embed the extrinsic parameters from the measurements in the pinch-off and active region. In consequence, only the intrinsic model needs to be considered when identifying the parameters of the equivalent circuit in the pinch-off and active regions.

Additionally, due to the symmetry of (9), the current source can be identified separately from the other elements, again simplifying the optimization procedure.

As the elements of the equivalent circuit can be assumed to change continuously with the applied voltages, the parameters computed for adjacent operating points have always been used as starting values to simplify the optimization.

A comparison of the obtained model with the original S-parameter measurements exhibits an excellent match.

Voltage dependent capacitances of the transistors are presented and compared with the data sheet, supporting the results.

CRediT authorship contribution statement

Martin Hergt: Visualization, Methodology, Formal analysis, Writing – original draft, Conceptualization. **Bernhard Hammer:** Software, Methodology, Conceptualization, Visualization, Validation, Writing – review & editing. **Martin Sack:** Methodology, Conceptualization, Writing – review & editing. **Lukas W. Mayer:** Conceptualization. **Sebastian Nielebock:** Funding acquisition. **Marc Hiller:** Methodology, Writing – review & editing, Conceptualization.

Declaration of competing interest

The authors declare that they have no known competing financial interests or personal relationships that could have appeared to influence the work reported in this paper.

Supplementary materials

Supplementary material associated with this article can be found, in the online version, at doi:10.1016/j.pedc.2025.100108.

Data availability

No data was used for the research described in the article.

References

650V Enhancement mode GaN transistor - GS66504B. *Data sheet, rev. 170321*, (2017)). GaN Systems. https://www.gansystems.com.

Endruschat, A., Novak, C., Gerstner, H., Heckel, T., Joffe, C., & März, M. (2018). A universal spice field-effect transistor model applied on SIC and GAN transistors. *IEEE Transactions on Power Electronics, 34*(9), 9131–9145.

Heckel, T.: Charakterisierung dynamischer eigenschaften und modellbildungen neuartiger leistungshalbleiterbauelemente auf basis von SIC und GAN. Dissertation, 2018.

Hergt, M., Mayer, L. W., Sack, M., Nielebock, S., & Hiller, M. (2019a). Power semiconductor characterization using pulse S-parameter measurements. PCIM Europe 2019. In *International exhibition and conference for power electronics, intelligent motion, renewable energy and energy management*. VDE.

Hergt, M., Mayer, L.W., Sack, M., Nielebock, S., & Hiller, M.: SiC diode characterization using pulsed S-parameter measurements. European conference on power electronics and applications (EPE'19 ECCE Europe) 2019b. Genova, Italy.

Hergt, M., Hammer, B., Mayer, L. W., Sack, M., Honsberg, M., Nielebock, S., & Hiller, M. (2024). Modelling and characterization of power semiconductors in the frequency domain. In *IEEE ECCE Europe 2024*. Darmstadt, Germany.

Jarndal, A. H. (2006). *Large-Signal modeling of Gan device for power amplifier design*. Kassel University Press GmbH. Dissertation.

Kompa, G. (1995). Modeling of dispersive microwave FET devices using a quasi-static approach. *International Journal of Microwave and Millimeter-Wave Computer-Aided Engineering, 5*(3).

Silicon Carbide Power. (2017). Silicon carbide power MOSFET C3M0120090J. *Data sheet, rev. 12-2015*. CREE. https://www.cree.com.